Evaluating actual Evapotranspiration using SEBAL model , in the omo kuraz irrigation site, Ethiopia.

Nigatu Toma (PhD candidate) [1], Tena Alamirew (PhD) [2], and Samuel Hatiye(PhD) [2,]*

1 Wolaita Sodo University collige of Engineering , Ethiopia; tomanigatu@yahoo.com

2 Water and Land Resource Center, Addis Ababa University, Ethiopia; tena.a@wlrc-eth.org

* Department of Water and Irrigation Engineering, Arbamich university, Ethiopia: samuelidagalo@gmail.com

Abstract:

The purpose of this study was to assess actual water use for different land uses particularly for agricultural crops is considered as one of the major factors for water resource planning and irrigation water management. However, actual water use of a sugar cane is mainly determined by its actual evapotranspiration (ETa). In order to analyze the distribution of evapotranspiration over the treatment area, the SEBAL (surface energy balance algorithm) model was used to evaluate the evapotranspiration (ET) rate for sugar cane at the lower reach of the omo river basin. Surface energy balance algorithm input like NDVI, and also along with actual field data (irrigation delivery schedule, root depth of crop in each stage, soil moisture before and after irrigation and water diverted to the field) in recent time, with the accomplishment of new satellite application, evapotranspiration can be calculated from remotely sensed land surface temperature using various land surface energy balance algorithms. In put parameter like: Land surface temperature, TOA albedo and emissivity was calculated from land sat 8 image using ENVI software. Meteorology data was collected from the farm site meteorology station. This especial method apply the collection of meteorological observation with data extracted from remote sensing to calculate evapotranspiration and other energy exchange at earth surface. The result shows that SEBAL (ETa) varies between 5 mm day-1 and 6mm day-1 in the study area. As a result, the researcher made the following recommendations: in the large scale irrigation farm remote sensing approach is very important to asses actual (ET) but there is some limitation in cause of potential (ET) estimation so other researcher should work on this again.

Keywords: *Evapotranspiration, SEBAL model, Remote sensing, Landsat 8*

Introduction

Surgical estimation of Evapotranspiration (ET) using remote sensing and image anlysis techniques requires understanding effects of the input parameters to the model and used satellite data on the accuracy of the results. References [1, 2] detailed the SEBAL model's fundamental concepts and summarized its accuracy across a variety of climatic circumstances at both field and watershed sizes in more than 30 nations around the world. The usual accuracy at the field scale was 85 percent for a single day and 95 percent on a seasonal basis. The yearly ET of big watersheds was determined to be 96 percent accurate. Based on the study's accuracy, the author stated that SEBAL may be utilized and executed to solve water resource and irrigation concerns. Similarly, Reference [3] investigated the impact of surface heterogeneity on SEBAL modeling performance. Landsat 8 was employed as a data source in the study. According to the findings, landscape heterogeneity influences remotely sensed projections of heat fluxes. Furthermore, Reference [4] examined the sensitivity of the SEBAL model parameters for mapping winter wheat ET in South China. Based on the fact that the SEBAL model works best in places with a high proportion of sunny days and a low level of pollution. Furthermore, References [5, 6] investigated the effects of dynamic input variables and satellite sensor spatial resolution on sensible heat flow (H) calculated using the SEBAL model. Reference [6, 7] did another major research on the SEBAL model, and they examined the theory of the SEBAL, which was initially created for Egypt, Spain, and Niger. From 2001 to 2007, the researchers calibrated and verified the SEBAL algorithm using photos from the semi-arid area of the Low-Middle Sao Francisco River basin in north-eastern Brazil. Among the metrics studied were surface albedo, surface temperature, atmospheric and surface emissivity, soil heat flux, surface roughness, net radiation, air temperature gradients, sensible heat flux, latent heat flux, evaporative fraction, and photosynthetically active radiation. According to the study's findings, it is critical to distinguish between immediate and daily time frames. For immediate values, the hot and cold pixel calibration has to be applied to each individual picture. The values of the instantaneous evaporative fraction have to be corrected for daily scale. The study also discovered that it is beneficial to utilize curves of the ratio of actual to reference evapotranspiration in calibration procedures rather than the average values of the pixel with the lowest and highest surface temperatures since this ratio varies throughout the year. Others attempted to improve on the initial SEBAL model in order to estimate Evapotranspiration more accurately. The improved surface energy balance method for land was shown in references [8, 9]. (M-SEBAL). SEBAL may be used to evaluate irrigation system performance, agriculture water production, and other natural resource uses. Reference [10] used remote sensing and GIS techniques to estimate water balance components in the arid-mountainous catchment of Manshad in Iran's Yazd region during 2006–2007.To estimate the actual Evapotranspiration across the research region, the SEBAL model was utilized. The water balance for the study region was evaluated using actual evapotranspiration, catchment runoff, and average precipitation. Using extremely high resolution aircraft remote sensing images, reference [11] evaluated the SEBAL model for mapping evapotranspiration. SEBAL results for irrigated fields with higher ET, little or no water stress, and full ground cover surfaces were clearly superior to those for dry land fields with lower ET, bigger soil water deficits, and sparser plant cover. This article evaluates the SEBAL model for estimating real evapotranspiration in the lower Omo basin kuraz irrigation, a dry region of Ethiopia. The study also creates an autonomous ENVI model for calculating SEBAL components.

Materials and Methods

Study area

The Omo Give River Basin was studied, which is located between latitude 3500'E and 3800'E and longitude 4030'N and 9030'N. The basin has a total area of 79000km^2 and an elevation range of 300-2800 meters (m). The Gibe River was known as the Omo River in its lower reaches, and the Omo River's general flow direction was southward towards the Turkan River in Kenya. It is a confined river basin that drains into Lake Turkana in Kenya, which serves as its southern boundary. The total mean yearly flow from the river basin was estimated to be approximately 16.6 billion cubic meters. Because of the variability in topography, rainfall, and land use, the basin has complex hydrological processes.

The project's location is in the Southern Nations Nationalities and Peoples Regional State (SNNP), which is located between latitude 3400' to 3800'E and longitude 400' to 800'N. It is located in the Omo-Gibe River Basin and falls in the South Omo zone's Selamago and Gnangatom Woredas, the Bench-Maji zone's Menit Shasha and Maji Woredas, and the Keffa zone's Decha Woreda. The area's geography was flat, with slopes of less than 2% in most places, which is ideal for mechanized commercial farming in general.The elevation ranges between 380 and 485 masl, the command area annual rainfall is in the range of 661.4 mm, the temperature over the project area varies from 190C (July and August) to 330C (February), the wind speed ranges from 10.4 km/h to 15.5 km/h, the humidity ranges from 57 percent to 75 percent, and the sunshine hours range from 6.9 hours to 10.2 hours. The average monthly evapo-transpiration ranges from 151mm to 205mm, with an annual value of 2 070mm.

The gross command area of the main systems, which is approximately 175,000 ha, has been chosen to analyze the performance of major irrigation systems (Fig. 1). Surface water is supplied by the irrigation system in the omo kuraz. The experimental location was located between

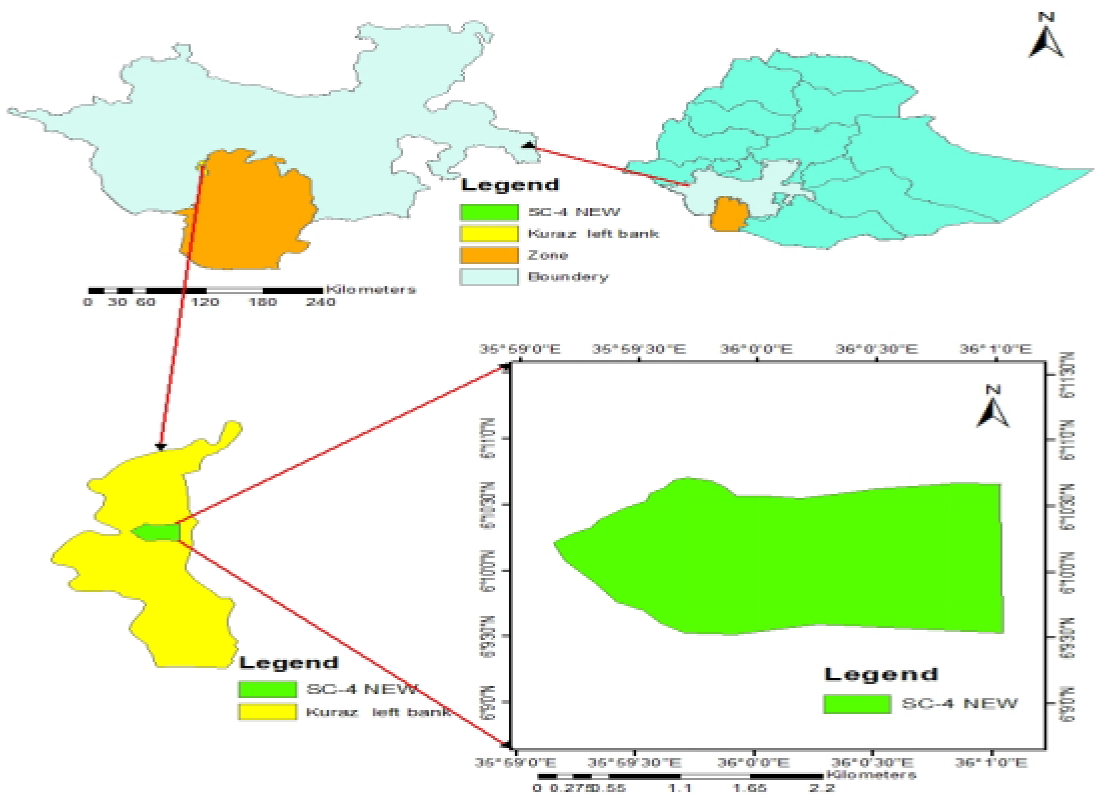

Fig 1 map of the study area.

Experimental site

The experiment was carried out in a sugar cane field by the researcher. As a result, he chose four treatments from the four stages of sugar cane development. For example, to measure the quantity of water diverted to the field and soil moisture, one treatment from the early stage (TE), one treatment from the planting stage (Tp), one treatment from the middle stage (TM), and one treatment from the harvesting stage (TH) were used. In addition, the researcher chose four furrows from each treatment to assess soil moisture and measure the amount of water diverted to the field. The length of each furrow (0, 1/4,1/2,3/4) has been used to measure the amount of water diverted to the field using a partial flume and soil moisture after and before irrigation using an auger. The experimental plot was situated in a single path and row over lap zone (170 and 56). Actual and potential evapotranspiration, on the other hand, were assessed using satellite images acquired by the land sat8 operational land imager sensor (L8-OLIS) and analyzed with ENVI software.

Surface Energy Balance Algorithm for Land (SEBAL) for evaluation **Evapotranspiration**

SEBAL is an image processing model that estimates actual ET by solving the terms of the surface energy balance derived from the visible, near-IR, and thermal-IR bands of the electromagnetic spectrum. More explanation about SEBAL model given by Reference [14].In the SEBAL model, ET is assessed from satellite images and climate data using the surface energy balance as illustrated in Fig. 1. Since the satellite image supply information for the overpass time only, SEBAL computes net radiation (Rn), sensible heat flux (H) and soil heat flux (G) for every pixel and the latent heat flux (LE) is acquired as a residual in energy balance equation

$$Rn = LE + H + G \tag{1}$$

Where LE latent heat is flux (ET in energy units), Rn is net radiation at the surface, H is sensible heat flux to the air, and G is soil heat flux (W m-2)

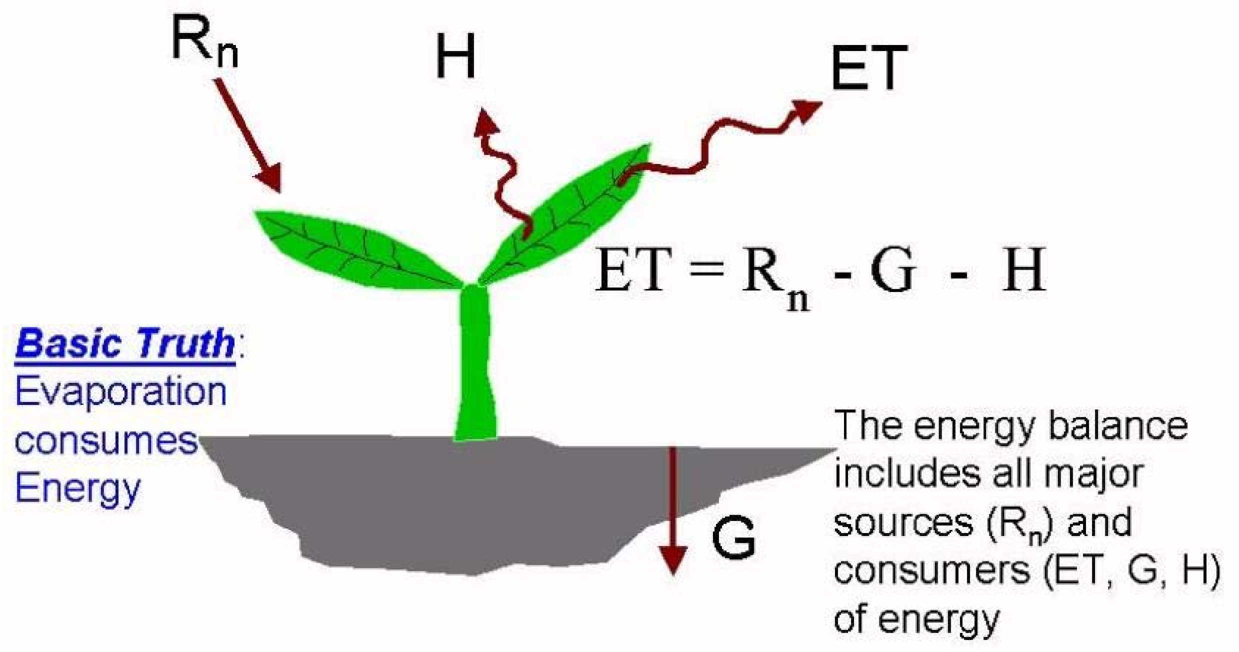

Figr 1 flow chart of latent heat of flux

A physically based one-layer sensible heat transfer system and an experimental estimation system for soil heat flux are combined in the practical SEBAL method. Surface temperature, surface albedo, and the normalized vegetation index (NDVI) were used as dependent variables to calculate the soil heat flux as an empirical fraction of net radiation. The net radiation was calculated using radiation's spatially variable reflectance and emittance. Rn was calculated as the sum of inward and outward radiation components.Net short-wave radiation was calculated using astronomical equations and estimates of atmospheric transmittance (τ_{sw}) and $\alpha_{0,}$ Incoming long wave radiation was modeled using overpass time and air temperatures (Ta), which were assumed to be constant over the area.

Ts and an estimate of surface emissivity (Ɛo) on the basis of NDVI were used to calculate outgoing long-wave radiation. Sensible heat flux (H) was the rate of heat loss to the air due to temperature variations via convection and conduction. Sensible heat flux (H) was calculated using the air density fraction, specific heat constant, temperature difference, and aerodynamic resistance. The energy budget is closed on a pixel-by-pixel basis by using λET as the residual of the energy budget equation. To determine its constitutive parameters, this method requires spectral radiance in the visible, near infrared, and thermal infrared regions of the spectrum: surface albedo (α_0), NDVI, and surface temperature (Ts).

$$R_n = (1-\alpha)R_s\downarrow + R_L\downarrow - R_L\uparrow - (1-\varepsilon_0)R_L\downarrow \quad (2)$$

Where, $Rs\downarrow$ is the incoming short-wave solar radiation, α is the surface short-wave albedo, $R_L\downarrow$and $RL\uparrow$are incoming and outgoing long-wave radiation (W/m^{-2}), εo is the land surface emissivity. Standard algorithms and/or land surface parameterization schemes are used to calculate all of this.

Surface albedo was defined as the ratio of solar electromagnetic radiation reflected from soil and plant surfaces to incoming radiation. Its value was calculated by combining the spectral reflectance values from Landsat 8 OLI's visible, near-infrared, and short-wave bands [15]. The surface albedo was calculated using the following equation:

$$\alpha = \frac{\alpha_{toa} - \alpha_{path-radiance}}{\tau_{sw}^2} \quad (3)$$

Where α _path radiance was the average of the fraction of solar incident radiance scattered to the sensor before reaching ground level for all bands. Its values range from 0.025 to 0.04, with 0.03 recommended for SEBAL [16]. Furthermore, τ_{sw} was the atmospheric transmissivity, which was calculated using the equation:

$$\tau_{sw} = 0.75 + 2 * 10^{-5} * Z \quad (4)$$

Where, Z was the height of the meteorological station from the mean sea level [17].

Surface albedo was computed by correcting the (α_{toa}) atmospheric transmissivity. The simplest method was proposed by Liang [18].

$$\alpha_{toa} = \frac{0.356\rho_2 + 0.130\rho_4 + 0.373\rho_5 + 0.085\rho_6 + 0.072\rho_7 - 0.0018}{0.356 + 0.130 + 0.373 + 0.085 + 0.072} \quad (5)$$

Whereas, ρ_2, ρ_4, ρ_5, ρ_6, ρ_7 band (2, 4, 5, 6 and 7) respectively from landsat8 image analysis. According to the liang(2000) $band_3$ was ignored during the evaluation of surface albedo (the green part of the spectrum).

The flux of direct and diffuse solar radiation that actually reaches the ground, assuming clear sky conditions, for the incoming short-wave radiation was calculated as the following equation [13] :

$$R_s \downarrow = S_c \cos\theta * d_r * \tau_{sw} \tag{6}$$

S_c denoted the solar constant, which is equal to 1367 (W/m^2). Cosθ was the cosine of the incident angle of solar radiation, which can be found in the satellite image header file (for Landsat8 data in OLI format). dr was calculated as the inverse of the square relative distance of the Earth to the Sun [13]:

$$d_r = 1 + 0.033\cos\left(\frac{2\pi}{365} J\right) \tag{7}$$

Where; J was the sequential day of the year.

The reflected long-wave radiation flux is calculated using Stefan-Boltzmann's relation as:

$$R_L \uparrow = \varepsilon_o \sigma T_s^4 \tag{8}$$

Where, ε_0 was the broadband surface emissivity, σ was the Stefan-Boltzmann constant (5.67 × 10^{-8} W/M^2/K^4) and T_s was the surface temperature (K) evaluated using ENVI software researcher was analyzed land sat 8 image [19].

The following equation was used to calculate the broad band surface emissivity:

$$\varepsilon_o = 0.004 * pv + 0.986 \tag{9}$$

$$pv = \left(\frac{NDVI - NDVI_{min}}{NDVI_{max} - NDVI_{min}}\right)^{\wedge}2 \tag{10}$$

Where, NDVI normalized difference vegetation index, $NDVI_{min}$ was normalized difference vegetation index at minimum condition, $NDVI_{max}$ was normalized difference vegetation index at maximum condition and pv was proportion of vegetation.

NDVI was calculated as the following equation [13].

$$NDVI = \frac{\rho_5 - \rho_4}{\rho_5 + \rho_4} \tag{11}$$

Where; ρ_5, ρ_4 were the spectral band 5, and band 4 respectively.

Incoming long wave radiation $R_L\downarrow$ radiation was the flux of thermal radiation from the atmosphere downwards, which was calculated using the Stefan-Boltzmann equations:

$$R_L\downarrow = \varepsilon_a \sigma T_a^4 \tag{12}$$

Where; T_a was the temperature of the air near the surface, and εa atmospheric emissivity [20]. The following equation was used to calculated atmospheric emissivity:

$$\varepsilon_a = 0.85(-\ln \tau_{sw})^{0.09} \tag{13}$$

Soil heat flux needed in SEBAL algorithm cannot be calculated directly from satellite images. Therefore, an mathematical equation was applied to estimate Go, which utilizes *NDVI* and Rn. The equation was

$$G_o = \left(0.30\left(1 - 0.98 NDVI^4\right)\right) R_n \tag{14}$$

This equation was derived from actual measurements as reported in [17]. According, [21], Equation (14) was applicable only to a vegetated land surface.

Sensible heat flux was defined as the rate of heat loss to the air owing to a temperature differential via convection and conduction. The classical equation for sensible heat flow was a function of temperature gradient, surface roughness, and wind speed, and this step is prone to failure owing to considerations and assumptions. The sensible heat flux is represented by the Equation (15):

$$H = \frac{\rho_a c_p dT}{r_{ah}} \tag{15}$$

where ρ_a=air density kg m^3; Cp=specific heat of air at constant pressure J kg^{-1} K^{-1}; and r_{ah}=aerodynamic resistances m1 between two near surface heights, z_1 and z_2, which are commonly 0.1 and 2 m determined as a function of the predicted aerodynamic roughness of the given pixel. The dT parameter (k^0) represents the difference in near-surface temperature between z_1 and z_2.

Allen [22] proposed a linear relationship between dT and Ts, whereas others [23] used a step function to calculate Ta from Ts values. A regression analysis was carried out in this study utilizing the Ta values obtained from the site meteorological stations and the radiometric LST obtained from the landsat8 image product. The resulting linear equation for the whole irrigation season is [24]:

$$dT(K^0) = -146.7055 + 0.5064T_s\ (K^0) \tag{16}$$

where, Ts(k^0) was surface temperature, dT was temperature difference at pixel.

The upright limits for describing sensible heat flux (H) and close surface vertical air temperature difference (Z_1 and Z_2, commonly 0.1 and 2.0 m above ground, respectively) were specified as reference heights (Z1 and Z2) (dTa). The sensible heat transfer equation then applies these restrictions to aerodynamic resistance (rah), as shown in [23]. The following equation [25] was used to determine (rah) using this method:

$$r_{ah} = \frac{\ln\left(\frac{Z_2}{Z_1}\right)}{u*k} \tag{17}$$

Where (z_2/z_1) denoted the reference height (z_2/z_1), k denoted the von Karmans constant (0.41), and u* denoted the fraction velocity.

The friction velocity (u*) at each pixel was calculated using observed wind speed measurements and the assumption that the wind speed at blending height was aerially constant (200m). Friction velocity (u*) was measured using the equation:

$$u* = \frac{k u_{200}}{\ln\left(\frac{200}{Z_{om}}\right)} \tag{18}$$

Where, u_{200} was the wind speed at the blending height (200m), k was the von karmans constant (0.41) and z_{om} was the length of surface roughness for momentum transport.

u_{200} is the wind speed at an assumed blending height of 200 m above the weather station [26] .

$$u_{200} = \frac{u_y \ln(67.8Z - 5.42)}{4.87} \tag{19}$$

Where, u_{200}(m/s) was the wind speed at blending height of 200m, u_y (m/s) was wind speed at the observed from weather station at 2m and z (m) was the elevation above sea level close to weather station.

The initial estimate of surface roughness length for momentum transport (Z_{om}) in the SEBAL method is based on the height of vegetation around the weather station (h) using an empirical equation [27].

$$Z_{om} = 0.12h \tag{20}$$

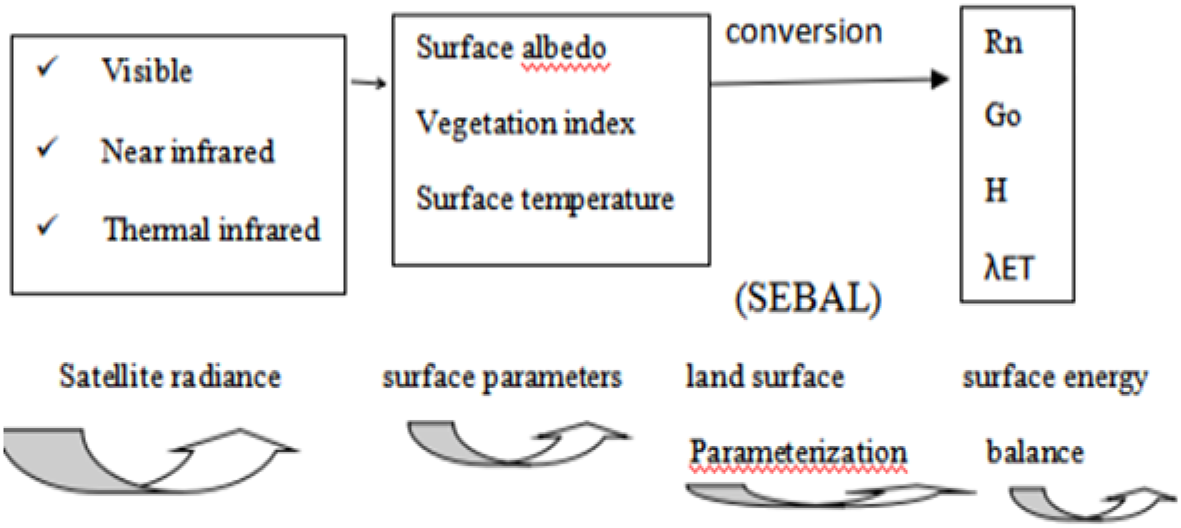

Fig2; flowchart of the research.

3. Results

Results and Discussion

3.1 Data used in calculation of irrigation performance indicators

Monthly and seasonal values of the V_c, P_g and P_e parameters needed to calculate the selected irrigation performance indicators were given in Table 1 for the 20018-2019 irrigation season.

Monthly and seasonal values of the ET_a parameters needed to calculate irrigation water management were shown in Tables 2 respectively, for the 2018-2919 irrigation season.

Dominant crops in omo kuraz sugar cane development project site were sugar cane. The total area of these sugar cane plantation, and irrigation irrigation system was surface irrigation was carried out with reference to these sugar cane. Crop areas for the 2018-2019 irrigation season in all experimental site indicated in the flowing table .

supply of water was evaluated at the diversion of field using the staff gauge. The depth of the water was evaluated and also the length of canal taken from research office of project. Then it was changed to mm by using Fancis formula then discharge evaluated.

Treatment	Length(m)	Oct H(cm)	Jun H(cm)	Apr H(cm)	July H(cm)	Area(ha)
Tp	1.3	37	41	21	37	27.93
TE	1.2	42	43	41	36	27.884
TM	1.2	36	39	20	20	15.11
Th	1.1	58	59	26	55	34.02

Radiometric correction of image

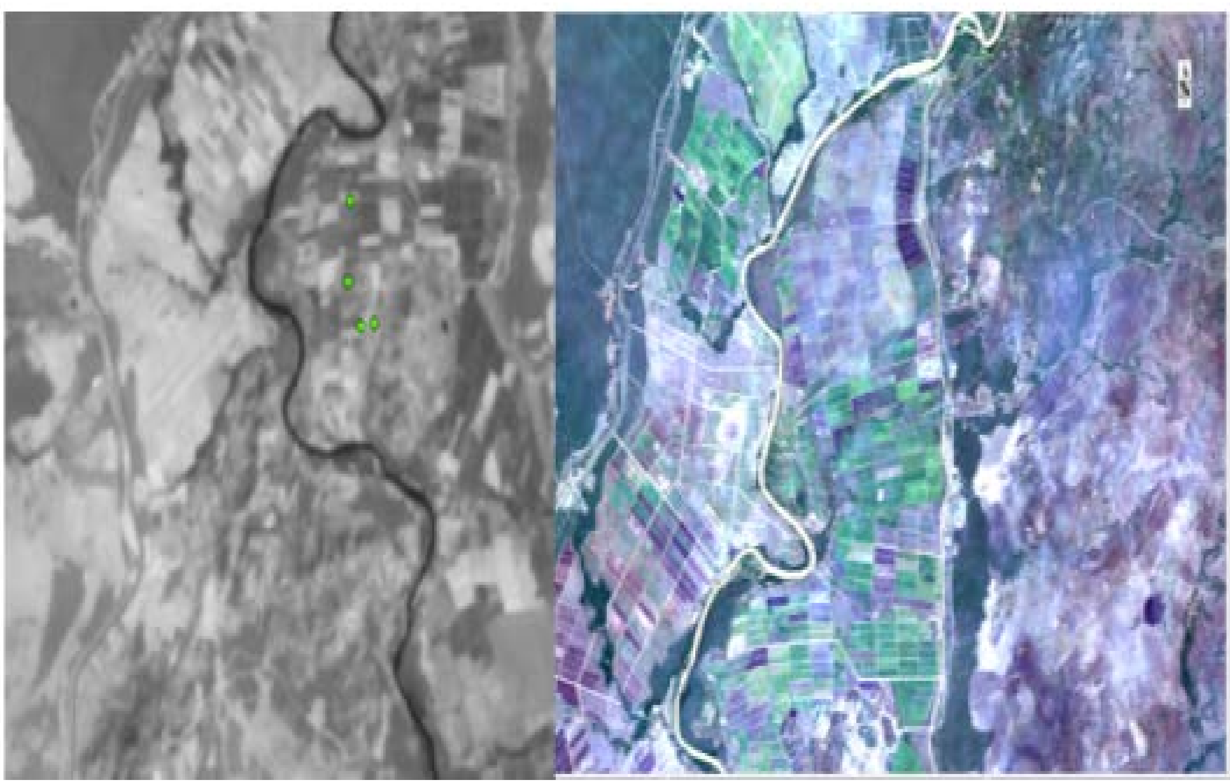

Figure 3. A screenshot of irrigation data input for the year 2018

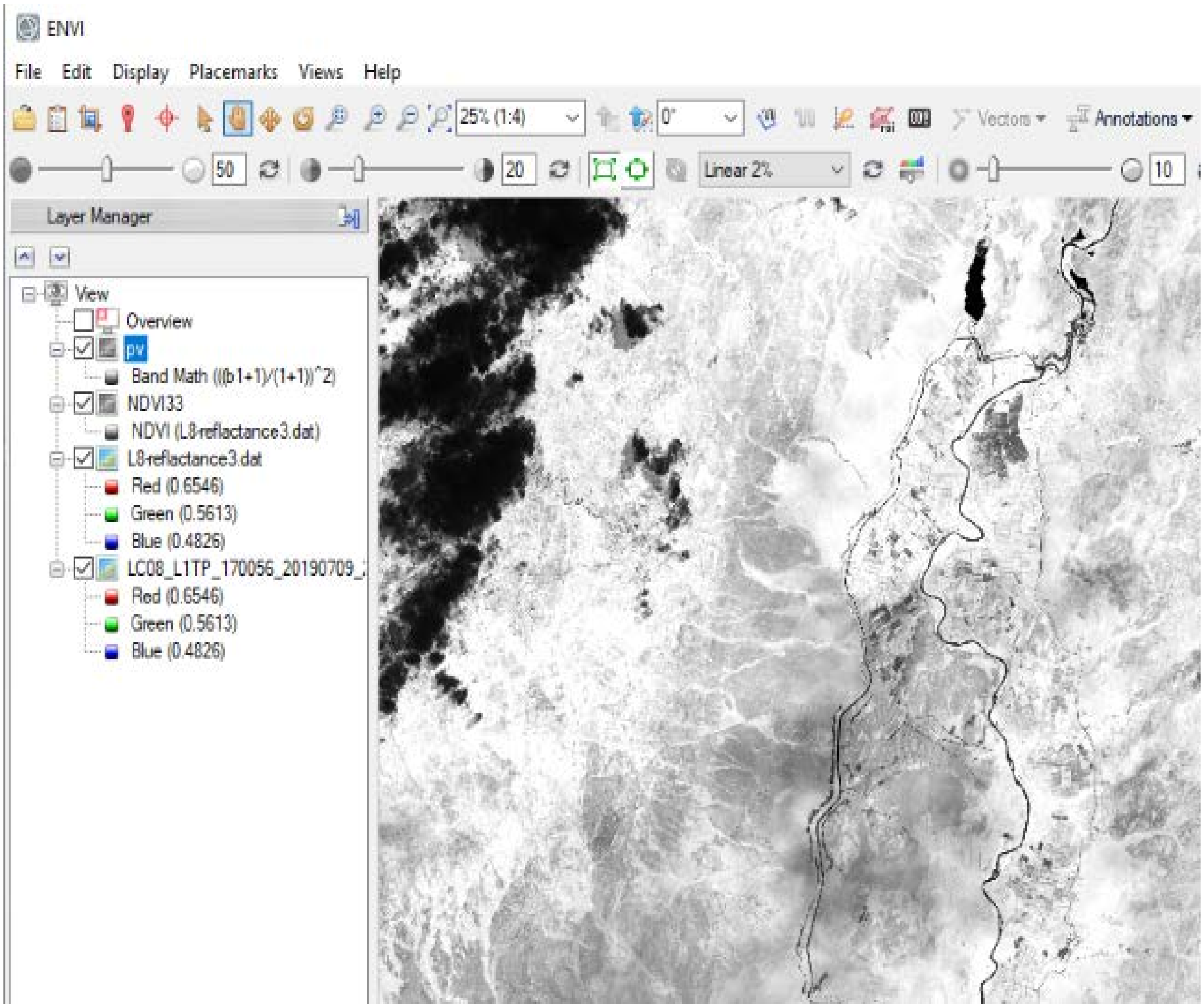

Figure 4 *A screenshot of irrigation data input for SEBAL* Pv value in study area.

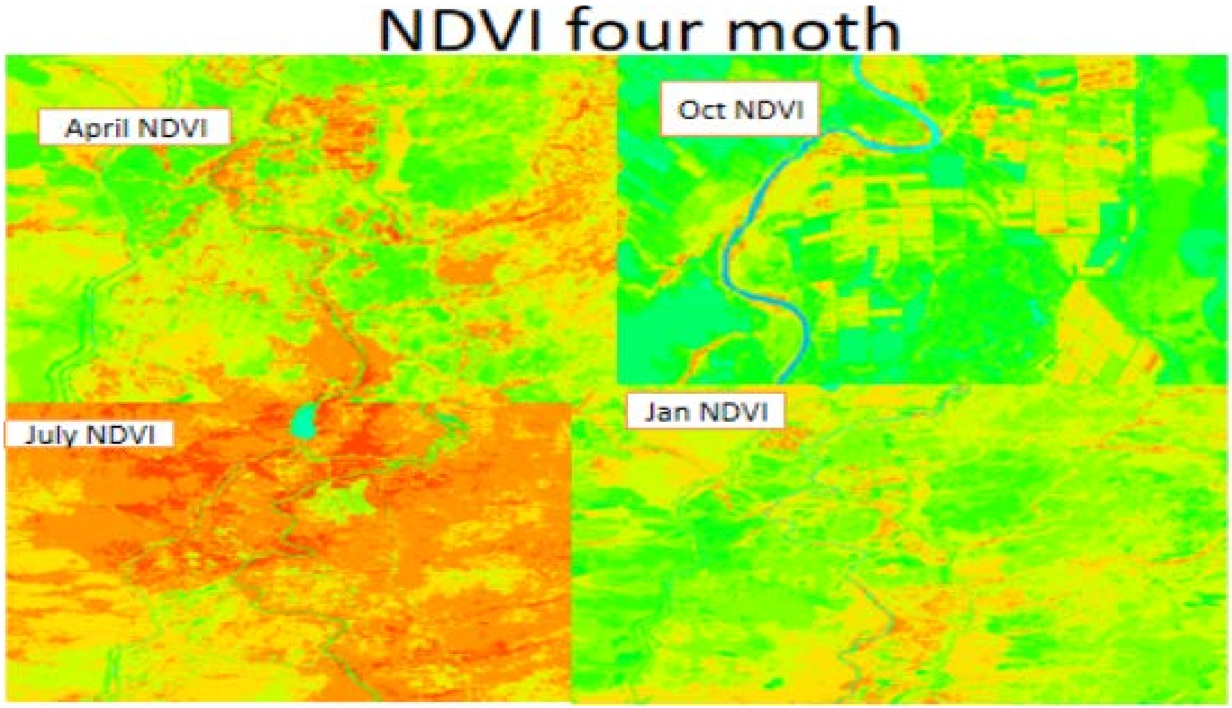

Figure 5 *A screenshot of irrigation data input for SEBAL* NDVI value in study area.

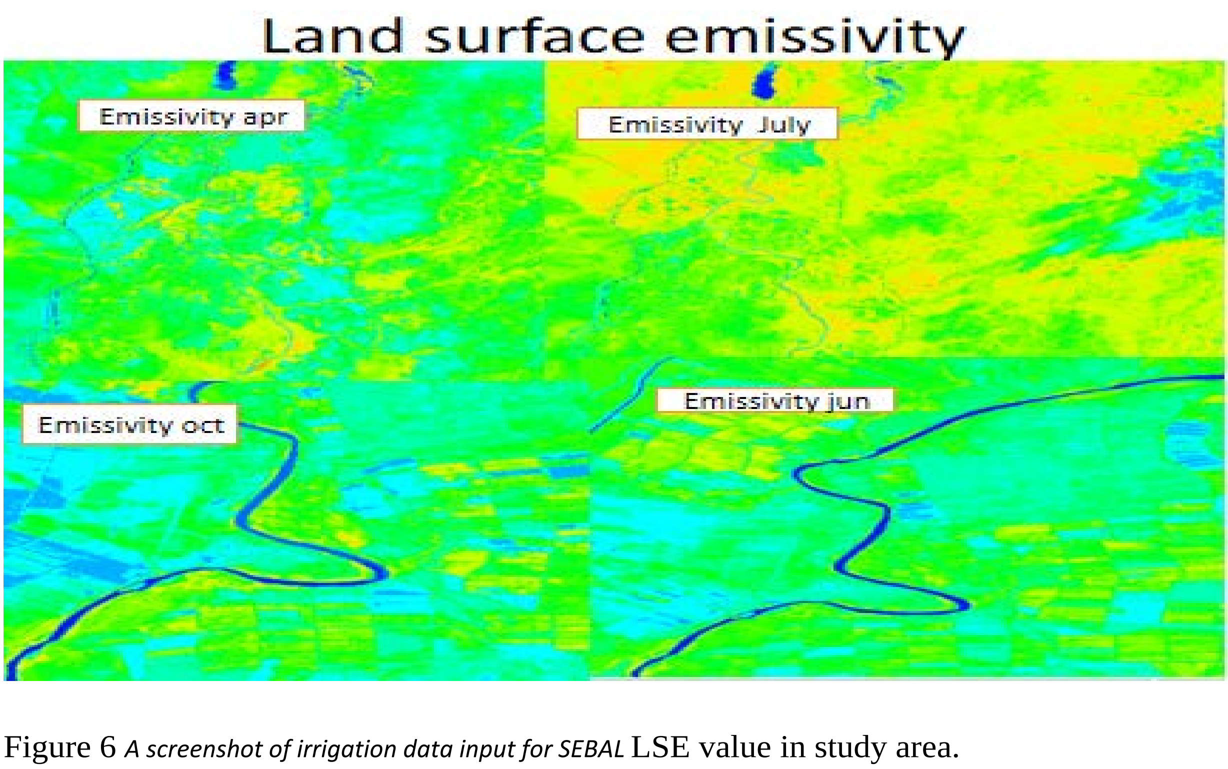

Figure 6 *A screenshot of irrigation data input for SEBAL* LSE value in study area.

Top of atmosphere albido

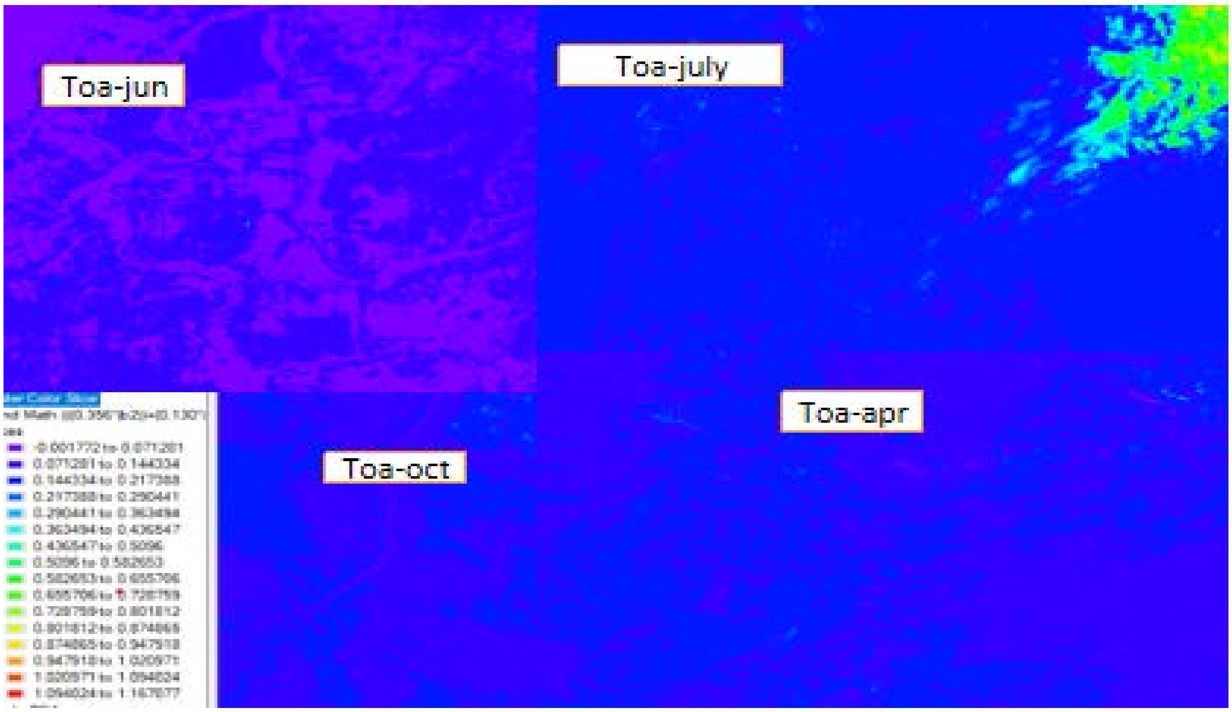

Figure 7 *A screenshot of irrigation data input for SEBAL* Top of atmospheric albido value in study area.

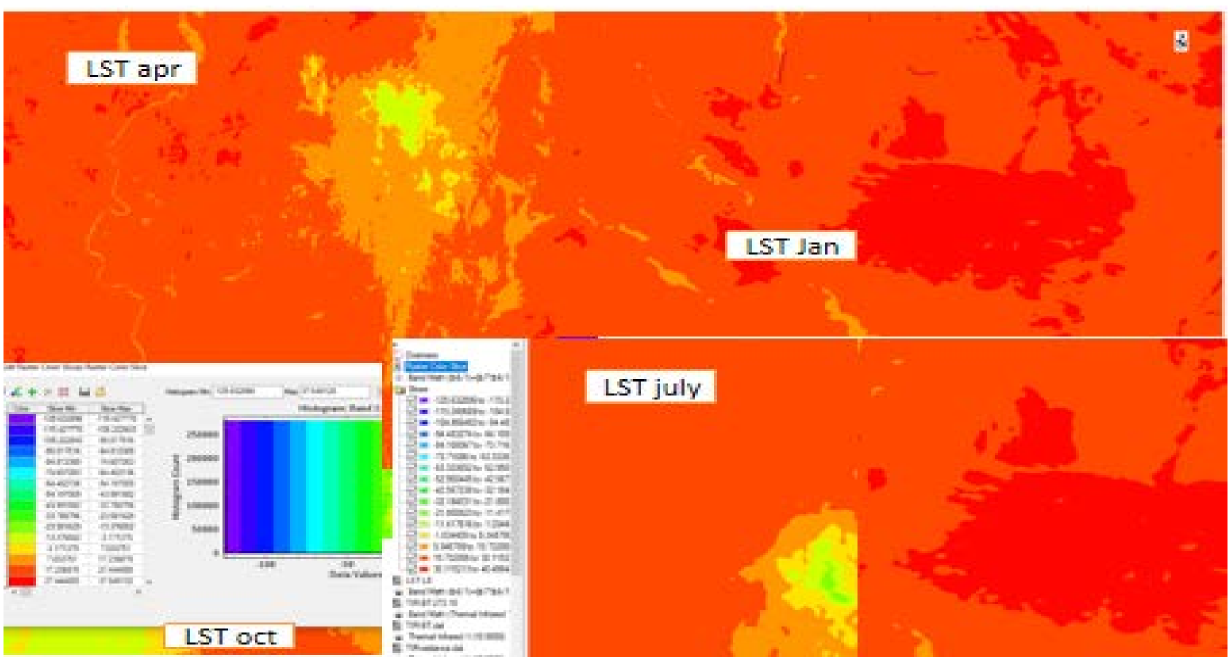

Figure 8 *A screenshot of irrigation data input for SEBAL LST* value in study area.

Table 1: Amount of the water diverted from source (V_c), total precipitation (P_g) and effective precipitation (P_e) parameters needed to calculate performance indicators during the 2018-2019 irrigation season.

Treatment(T) site	Water diverted from regulator, Vc(mm)				
	Oct	June	April	July	total
T_P	258	298	102	256	
T_E	274	285	170	220	
T_M	281	300	114	114	
T_H	270	313	64	213	
P_g(mm)	27.3	0	285.3	48.3	
P_e (mm)	26.1	0	153.5	44.6	

Table 2. Values of monthly and seasonal actual evapotranspiration (ETa) during the 2018-2019 irrigation season.

Treatment(T)	ETa(mm)				
	Oct	Jan	April	July	total
T_P	168	172	177	168	
T_E	174	169	170	150	
T_M	180	172	172	156	
T_H	171	168	177	156	
Average (mm)					

in table 2 ET_a values vary among pixels due to variation in the crop pattern, vegetative growth and poor irrigation management.

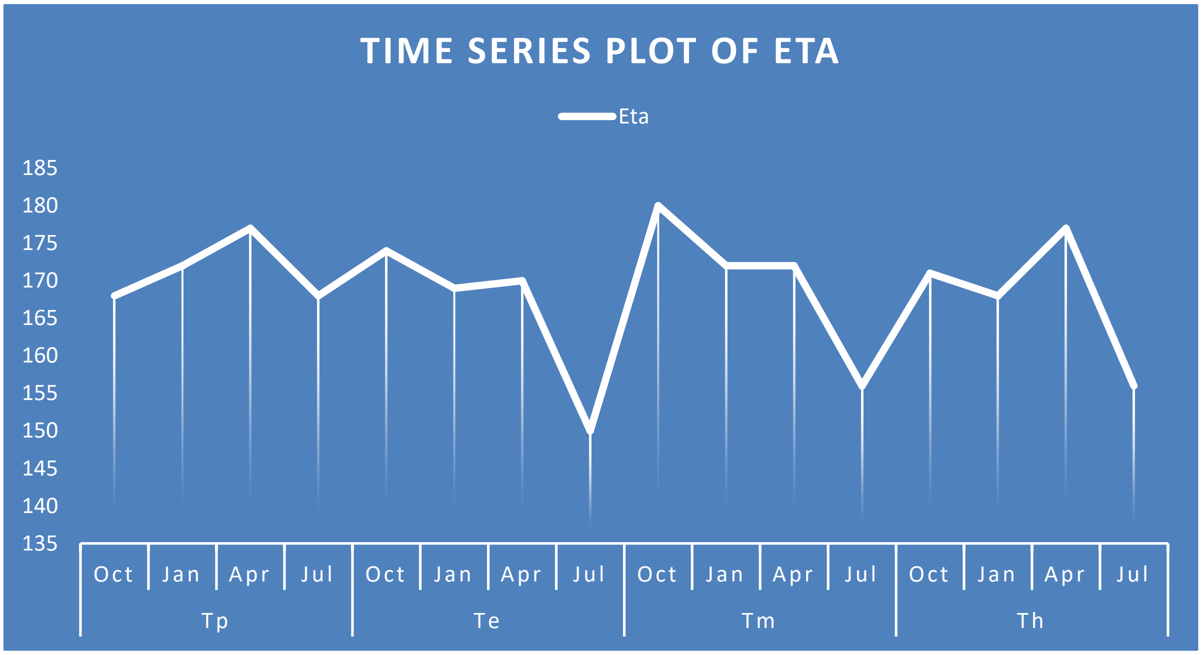

Figure 9 *time series plot of ETa value evaluted using SEBAL* model in study area.

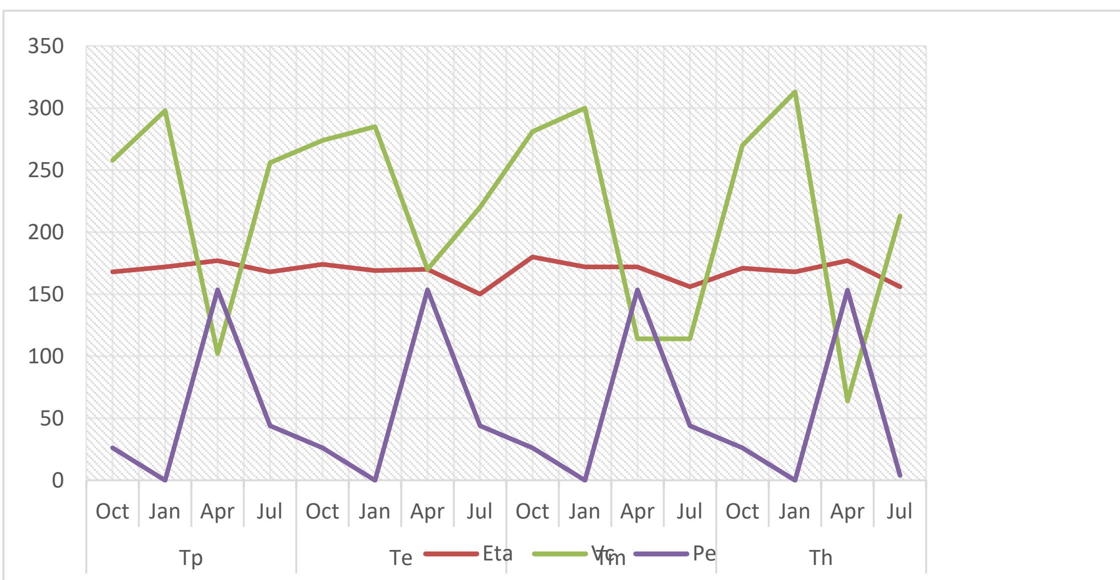

Figure 10 dynamical analysis of ETa value evaluted using SEBAL model with volume of water that diverted to the field in study area.

Conclusion

The purpose of this study was to investigate the SEBAL approach for mapping the geographical variance of real evapotranspiration across the Doon Valley region. The approach estimates ET on the day of satellite flyover using optical satellite images and the SEBAL algorithm. The real evapotranspiration (ET) was calculated using the SEBAL mode and its spatial variation was examined across different land coverings. When compared to other growth stage fields, agriculture terrace has the highest real evapotranspiration (6 mm day-1). However, the technique proposed that in the situation of inadequate ground-based hydrological data, SEBAL technology may serve as a rapid tool to estimate ET, and the ensemble of ET throughout a year can be used to efficiently plan water resources.Though this study only demonstrated one application of the SEBAL approach utilizing satellite imagery, future studies may necessitate ground validation of this technique employing a network of field lysimeters and calibrating hydrological models in ungauged watersheds using ET values as observable variables.

References

[1] E. Noordman,W. Bastiaanssen, H. Pelgrum, G. Davids, B. Thoreson and R. Allen, "SEBAL model with remotely sensed data to improve waterresources management under actual field conditions," J. Irrig. Drain. Eng., 2005.

[2] T. R. McVicar, J. D. Kalma, and M. F. McCabe, "Estimating land surface evaporation: A review of methods using remotely sensed surface temperature data," Surv. Geophys., vol. 29, pp. 421-469, 2008.

[3] X. Zhang, T. Berhane and G. Seielstad, "Comparision of landsat and MODIS estimates of heat fluxes: Effect of surface heterogeniety," in Geoscience and Remote Sensing Symposium, 2008. IGARSS 2008. IEEE International, 2008, pp. III- 759-III-762.

[4] X. Zhang and H. Wu, "Sensitivity analysis of the sunshine duration parameters in SEBAL model for estimating winter wheat evapotranspiration," in Geoscience and Remote Sensing Symposium (IGARSS), 2011 IEEE International, 2011, pp. 3350- 3353.

[5] D. Long, V. P. Singh and Z. Li, "How sensitive is SEBAL to changes in input variables, domain size and satellite sensor?" Journal of Geophysical Research: Atmospheres (1984–2012), vol. 116, 2011.

[6] A. d. C. Teixeira, W. Bastiaanssen, M. Ahmad and M. Bos, "Reviewing SEBAL input parameters for assessing evapotranspiration and water productivity for the Low-Middle São Francisco River basin, Brazil: Part A: Calibration and validation," Agric. for. Meteorol., vol. 149, pp. 462-476, 2009.

[7] R. Trezza, Evapotranspiration using a Satellite-Based Surface Energy Balance with Standardized Ground Control. Utah State University, Department of Biological and Irrigation Engineering, 2002.

[8] D. Long and V. P. Singh, "A modified surface energy balance algorithm for land (M-SEBAL) based on a trapezoidal framework," Water Resour. Res., vol. 48, 2012.

[9] C. G. Morton, Development and Application of an Automated Calibration Algorithm for Estimating Evapotranspiration from Agriculture using a Remotely Sensed Surface Energy Balance Model. UNIVERSITY OF NEVADA, RENO, 2011.

[10] M. T. Dastorani and S. Poormohammadi, "Evaluation of water balance in a mountainous upland catchment using SEBAL approach," Water Resour. Manage., vol. 26, pp. 2069-2080, 2012.

[11] G. Paul, Evaluation of Surface Energy Balance Models for Mapping Evapotranspiration using very High Resolution Airborne Remote Sensing Data, 2013.International Journal of Applied Engineering Research ISSN 0973-4562 Volume 11, Number 6 (2016) pp 3950-3955

© Research India Publications. http://www.ripublication.com 3955

[12] C. Wu, C. Cheng, H. Lo and Y. Chen, "Application of SEBAL and Markov models for future stream flow simulation through remote sensing," Water Resour. Manage., vol. 24, pp. 3773-3797, 2010.

[13] M. Tasumi, R. Allen, R. Trezza, R. Waters and W. Bastiaanssen, "SEBAL (Surface Energy Balance Algorithms for Land)," Advance Training and Users Manual–Idaho Implementation, Version, vol. 1, pp. 97, 2002.

[14] A. Tegos, A. Efstratiadis and D. Koutsoyiannis, "A parametric model for potential evapotranspiration estimation based on a simplified formulation of the Penman-Monteith equation," Evapotranspiration–An Overview (Edited by S.Alexandris), InTech, 2013

[15] Allen RG Using the FAO-56 dual crop coefficient method over an irrigated region as part of an evapotranspiration intercomparison study. *Journal of hydrology*. 2000b; *229*(1-2): 27-41.

[16] Bastiaanssen WGM SEBAL-based Sensible and Latent Heat Fluxes in the Irrigated Gediz Basin, Turkey. Journal of hydrology. 2000; 229(1): 87-100.

[17] Bastiaanssen WGM, Menenti M, Feddes RA and AAM Holtslag A Remote Sensing Surface Energy Balance Algorithm for Land (SEBAL): Part 1: Formulation. Journal of hydrology, (1998a) 212, 198-212.

[18] Stone LR, Schlegel AJ, Gwin Jr RE and AH Khan Response of corn, grain sorghum, and sunflower to irrigation in the High Plains of Kansas. Agricultural Water Management. 1996; 30(3): 251-259.

[19] Bastiaanssen WGM, Noordman EJM, Pelgrum H, Davids G, Thoreson BP and RG Allen SEBAL model with remotely sensed data to improve water-resources management under actual field conditions. *Journal of irrigation and drainage engineering*. 2005; *131*(1): 85-93.

[20] Sun Z, Wei B, Su W, Shen W, Wang C, You D and Z Liu Evapotranspiration estimation based on the SEBAL model in the Nansi Lake Wetland of China. *Mathematical and Computer Modelling*. 2011; *54*(3-4): 1086-1092.

[21] Li S and W Zhao Satellite-based actual evapotranspiration estimation in the middle reach of the Heihe River Basin using the SEBAL method. *Hydrological Processes*. 2010; *24*(23): 3337-3344.

[22] Allen RG, Tasumi M, Morse A, Trezza R, Wright JL, Bastiaanssen W and CW Robison Satellite-based energy balance for mapping evapotranspiration with internalized calibration (METRIC)-Model.. *Journal of irrigation and drainage engineering*. 2007a; 133(4): 395-406.

[23] Farah HO and WG Bastiaanssen Impact of spatial variations of land surface parameters on regional evaporation: a case study with remote sensing data. *Hydrological processes*. 2001; *15*(9): 1585-1607.

[24] Alexandridis TK, Cherif I, Chemin Y, Silleos GN, Stavrinos E and Zalidis GC. Integrated methodology for estimating water use in Mediterranean agricultural areas. *Remote Sensing*, (2009) *1*(3): 445-465.

[25] Shoubo Li and Wenzhi Zhao, Satellite- based actual evopotranspiration estimation in the middle reach of the Heihe River Basin using the SEBAL methods, (2010) .

[26] Allen RG, Pereira LS, Raes D and M Smith Crop evapotranspiration-Guidelines for computing crop water requirements-FAO Irrigation and drainage paper 56. *Fao, Rome*. 1998; *300*(9): D05109.

[27] Waters R, Allen R, Bastiaanssen W, Tasumi M and R Trezza Sebal. *Surface Energy Balance Algorithms for Land. Idaho Implementation. Advanced Training and Users Manual, Idaho, USA*. 2002; 9-28